Supporting Information for

Small Molecules Control the Formation of Pt Nanocrystals: A Key Role of Carbon Monoxide in the Synthesis of Pt Nanocubes

Binghui Wu, Nanfeng Zheng* and Gang Fu*

State Key Laboratory for Physical Chemistry of Solid Surfaces and Department of Chemistry, College of Chemistry and Chemical Engineering, Xiamen University, Xiamen 361005, China

Email: nfzheng@xmu.edu.cn, gfu@xmu.edu.cn (for DFT calculations)

Experimental Details

Reagents: The synthesis was carried out using commercially available reagents. Platinum(II) acetylacetonate [$Pt(acac)_2$, Pt 48.0% min] was purchased from Alfa Aesar, Oleylamine (OAm, 80-90%) from Acros Organics, Oleic acid (OLA) from Guangdong Xilong Chemical Co. Ltd., n-butylamine from Sinopharm Chemical Reagent Co. Ltd. (Shanghai, China). CO (99.99%) was purchased from Linde Gas. All chemicals were used as received without further purification.

Synthesis of Pt in mixed OAm and OLA: nanodendrites and 10.3-nm nanocubes

10.3-nm Pt nanocubes: 20mg $Pt(acac)_2$ was dissolved in a mixed solvent of 8mL OAm and 2mL OLA in 50-60°C water bath for 10min, then dipped into oil bath which was preheated to 180-190°C and stirred at 180°C with a CO flow (~30mL/min) for 40-60min. The black dispersion was then cooled down to room temperature. Pt nanocubes were precipitated out and washed twice with cyclohexane-ethanol. The precipitates were re-dispersed in 2mL of cyclohexane.

Pt nanodendrites were synthesized under the same condition above but without the CO flow.

Synthesis of Pt nanoparticles in pure OAm: polyhedral nanoparticles and nanocubes

5.0-nm polyhedral Pt nanoparticles: 20mg $Pt(acac)_2$ was dissolved in 10mL OAm in 50-60°C water bath for 10min, then dipped into oil bath which is preheated to 180°C and stirred at 180°C with a CO flow(~30mL/min) for 40-60min. The black dispersion was then cooled down to room temperature. Pt nanoparticles were precipitated out and washed twice with cyclohexane-ethanol. The precipitates were re-dispersed in 2mL of cyclohexane.

5.1-nm Pt nanocubes were synthesized under the same condition above, but using 1 atm CO gas instead of CO flow. Similarly, by using 2-atm CO, **4.1-nm Pt nanocubes** can be made.

Surface treatment of 10.3-nm Pt nanocubes

10.3nm Pt nanoparticles were treated according to Yang's report.[1] Pt nanoparticles were dispersed in n-butylamine at a concentration of 1mg-particles/mL. The mixture was kept under stirring for 3 days and then collected by using a centrifuge at a rate of 8000 rpm for 2 min. The precipitate was re-dispersed in 10 mL methanol by sonicating for 15 min and then separated by centrifugation. This procedure was repeated three times. The final samples were dispersed in ethanol for further characterization.

Characterization. Transmission electron microscopy (TEM) studies, including high-resolution TEM (HRTEM), were performed on a Tecnai F-30 high-resolution transmission electron microscope operating at 300 kV. X-ray diffraction (XRD) measurements were recorded on a PANalytical X'pert PRO diffractometer using Cu Kα radiation, operating at 40 kV and 30 mA. The XRD patterns of 3D randomly oriented assemblies of Pt nanoparticles were performed on dried powers of Pt nanoparticles deposited on a glass substrate. Pt dispersions were dropped on a surface-polished Si<100> wafer by

slow evaporation of cyclohexane to achieve the oriented assembly. The samples for IR spectra measurements were obtained by depositing the cyclohexane dispersion of Pt nanocubes on CaF_2 substrate followed by solvent evaporation.

Electrochemical Measurements. Before electrochemical analysis, the as-prepared Pt nanoparticles were treated with n-butylamine to replace the capping agents.[1] The concentration of nanoparticles was adjusted to 2.5 $mg \cdot mL^{-1}$ in ethanol, and 10 μL of the solution was then dropped onto a glassy carbon electrode. After ethanol evaporation under an infra-red lamp for several minutes, 10μL of 0.1 wt% Nafion solution was dropped on the electrode surface to cover and stabilize the nanoparticle assembly on the electrode surface. The Pt loaded glassy carbon electrode was immersed into 0.5 M H_2SO_4 as a working electrode. A saturated calomel electrode (SCE) and a platinum wire were used as the reference and counter electrode, respectively.

As shown in Figure S5a, cyclic voltammetry(CV) was measured at room temperature with potential scanned from 0 V to 0.5 V versus the normal hydrogen electrode, NHE. The CV of n-butylamine-treated 10.3 nm Pt cube showed a peak at 0.252V which originates from the hydrogen desorption on the Pt(100) face.[2,3] This result suggests that the {100}A facets are dominant in the 10.3 nm Pt nanocube, which is consistent with the TEM and XRD analyses(Figure 1c and 1d). This result also shows that the surfactants have been successfully removed by the n-butylamine-exchanging treatment. Before the butylamine treatment, only featureless CV curve was obtained.

As the surface of Pt nanocubes was accessible after n-butylamine exchanging, Pt nanocubes showed high activity in the electrocatalytic oxidation of methanol and formic acid.

CV of 10.3-nm Pt nanocubes was measured in 0.5 M H_2SO_4+0.25 M CH_3OH or 0.5 M H_2SO_4+ 0.5 M HCOOH solution at room temperature with potential scanned from -0.21 V to 0.9 V versus SCE at a scan rate of 200 $mV \cdot s^{-1}$. The maximum current densities of 10.3 nm Pt nanocubes were measured as 193 and 137 mA/mg, respectively (Figure S5b).

Computational details: The spin-polarized DFT calculations were carried out by using the Vienna ab initio simulation package (VASP).[4,5] The valence electrons were described by plane wave basis sets with a cutoff energy of 400 eV, and the core electrons were replaced by the projector augmented wave pseudopotentials.[6,7] The exchange-correlation functional utilized was the local density approximation with generalized gradient correction, GGA-PBE. The Pt(100) and Pt(111) surfaces were modeled by a 2×2 supercell with a five-layer slab and a vacuum region of more than 30 Å thickness. The top two layers of the slab and adsorbates were relaxed up to residual forces of less than 0.02 eV/Å, while the atoms in the bottom three layers were fixed in their bulk positions. For simplification, all adsorbates were placed on top sites over the surfaces. The k-points sampling was generated following the Monkhorst-Pack procedure with a 5×5×1 mesh. Calculations for the free gas-phase molecules were performed in a 20×20×20 $Å^3$ unit cell and the Brillouin zone was sampled by single k point.

The adsorption energy (E_{ads}) was defined as

$$E_{ads}=E_{slab/mole}-E_{slab}-E_{mole} \quad (1)$$

in which $E_{slab/mole}$ is the energy of the slab with adsorbates; E_{slab} is the energy of the slab, and E_{mole} is the energy of gas-phase molecular. Similar to Tang's work,[8] the surface energy (φ) for a give clean surface is calculated by

$$\varphi_{surf}= [(E_{slab}-nE_{bulk})-(E_{prim}-nE_{bulk})/2]/N_{surf} \quad (2)$$

where E_{bulk} is the energy of a bulk unit cell; E_{prim} is the energy of the slab as mentioned above but without any relaxation, i.e. all atoms frozen in bulk-truncated positions. N_{surf} is the number of the surface Pt atoms in the slab and n is a factor which equal to the atoms in slab unit cell divide by the atoms in bulk unit cell. For the surface covered by adsorbate, φ is calculated as:

$$\varphi_{ads} = \varphi_{surf} + E_{ads} \quad (3)$$

Table S1. Calculated adsorption energies and surface energies for Pt (100) and (111) facets before and after the adsorption of RNH_2 and/or CO

Adsorbants*	Converage	Adsorption energy (eV)		Surface energies (eV/atom)		
		E_{ads} (100)	E_{ads} (111)	φ_{100}	φ_{111}	$\Delta\varphi_{(100)-(111)}$
clear surface	-	-	-	0.90	0.64	0.26
RNH_2	0.25ML	-0.99	-0.75	0.66	0.46	0.20
CO	0.25ML	-2.03	-1.60	0.40	0.25	0.15
RNH_2/CO	0.25ML/0.25ML	-2.77	-1.66	0.21	0.23	-0.02
RNH_2-CO	0.25ML	-1.69	-1.41	0.48	0.29	0.19

* R=C_8H_{17} (n-octyl), ML = monolayer

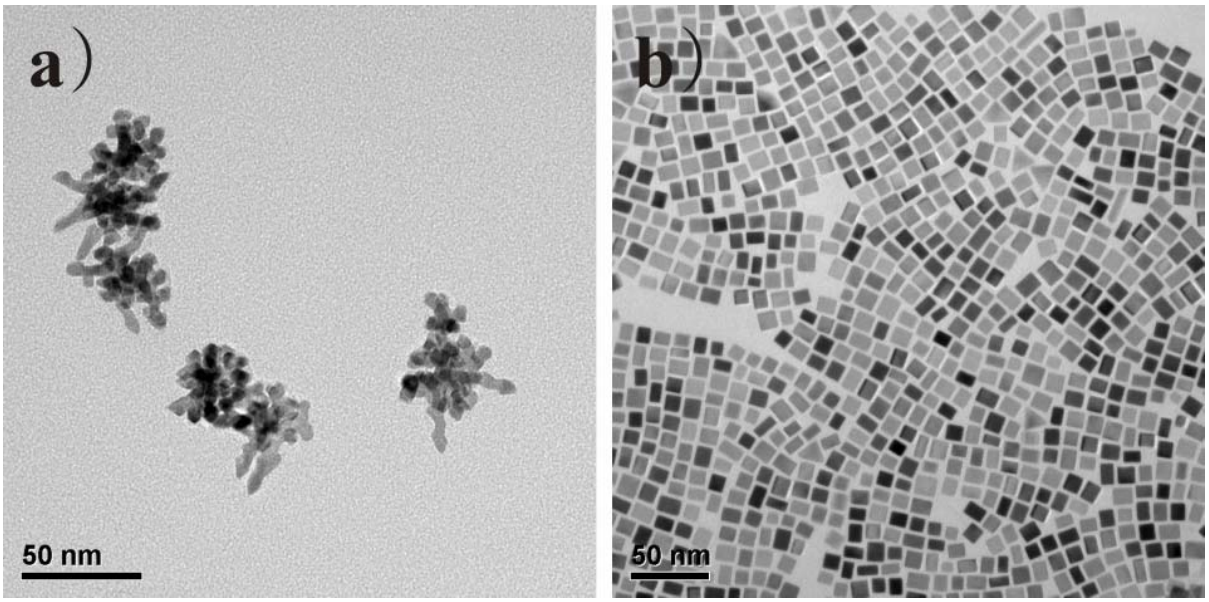

Figure S1. TEM images of a) Pt nanodendrites synthesized without CO and b) 10.3-nm Pt nanocubes under CO flow, both using OAm and OLA (volume ratio 4:1) as solvent at 180°C.

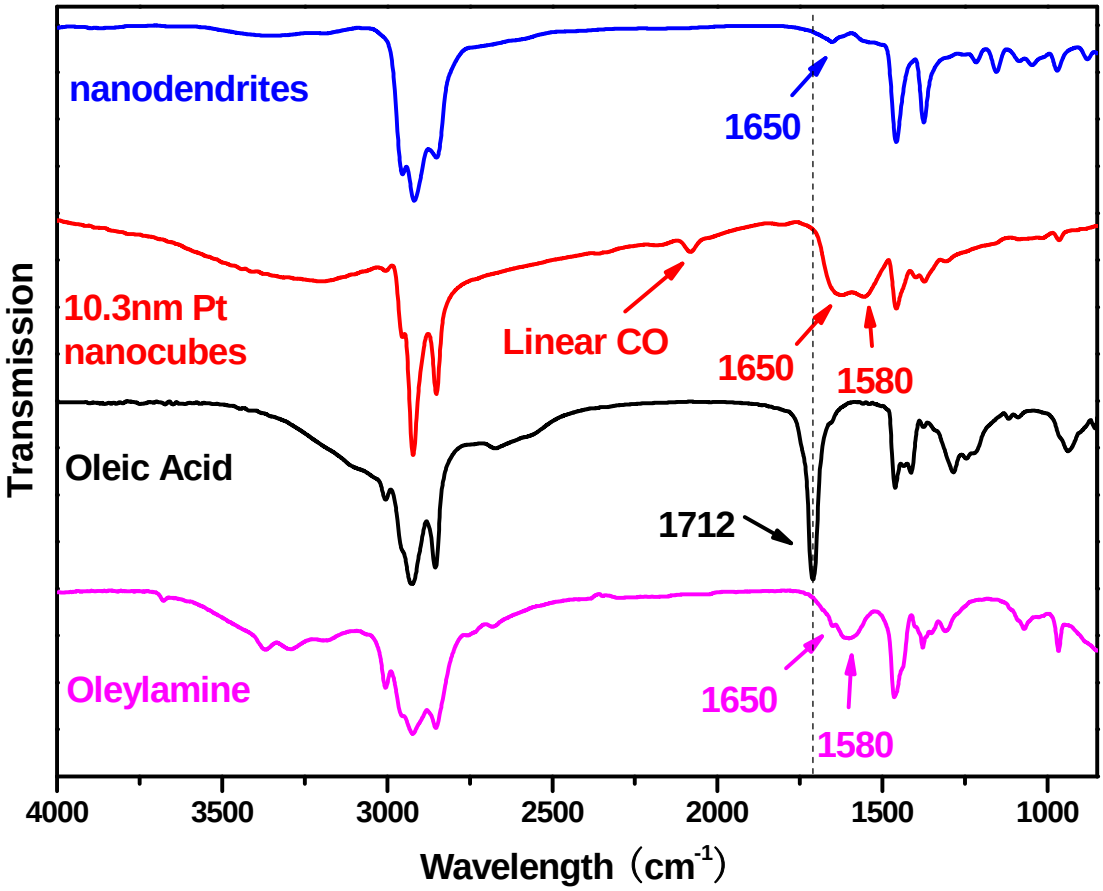

Figure S2. FT-IR spectra of the as-synthesized nanodendrites, 10.3-nm Pt nanocubes, OLA, and OAm.

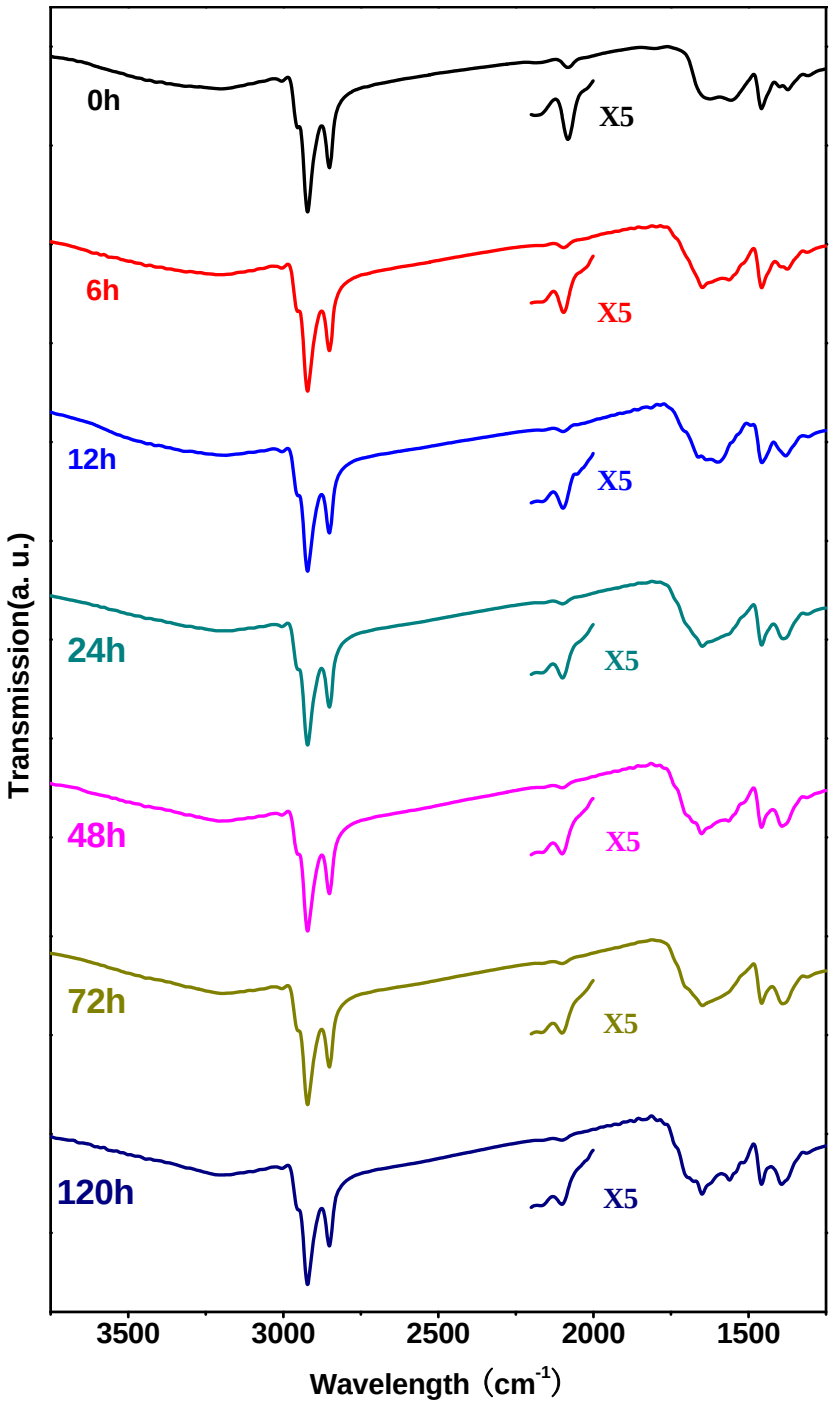

Figure S3. Time dependent FT-IR spectra of the as-synthesized 10.3nm Pt nanocubes after depositing their cyclohexane dispersion on a CaF_2 substrate. Although the IR peaks for CO gradually weakened over time, the strong CO adsorption was still observed on the Pt nanocubes after 120-h exposure in air.

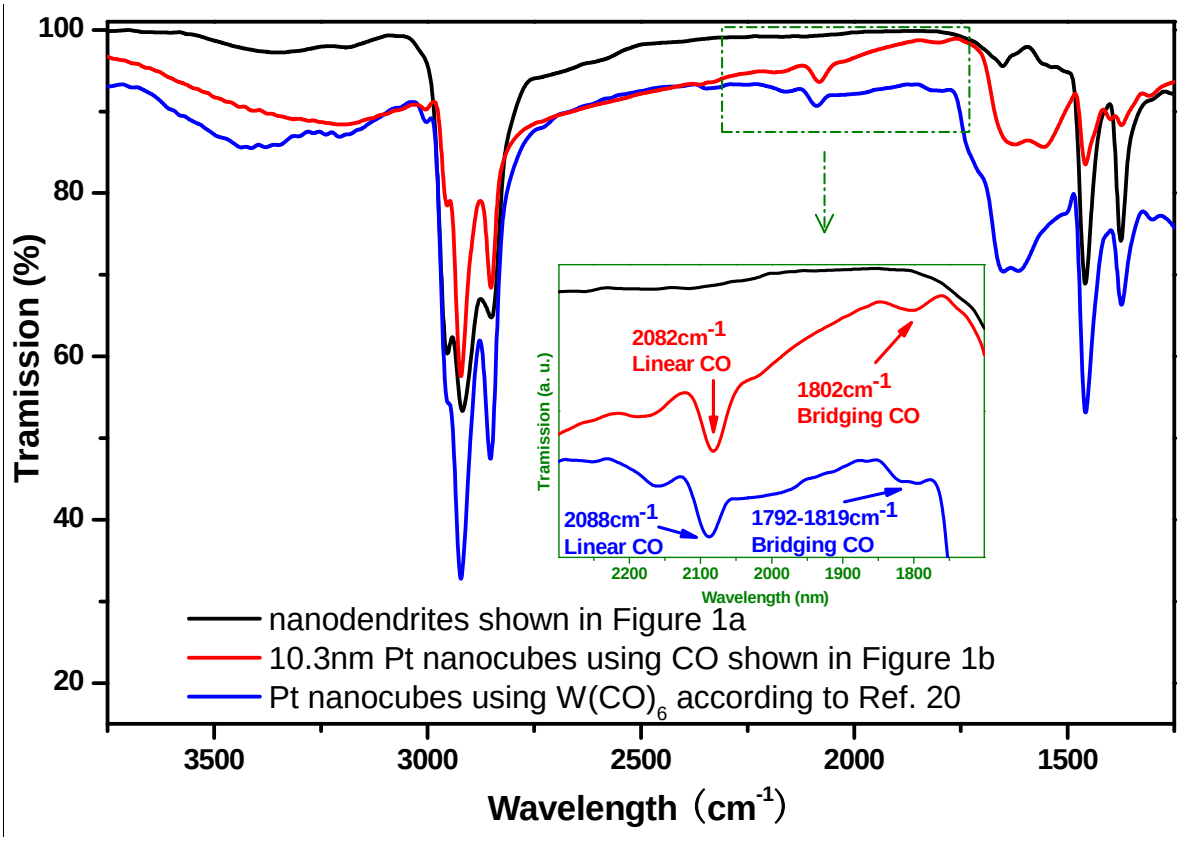

Figure S4. FT-IR spectra of the as-synthesized nanodendrites, 10.3-nm Pt nanocubes, and Pt nanocubes synthesized by using $W(CO)_6$ according to Ref. 20. The freshly prepared Pt nanocubes using CO displayed an obvious ν_{CO} band at 2082 cm^{-1} and a weak band at 1802 cm^{-1}, attributed to linear and bridging CO respectively. The Pt nanocubes that were prepared in the presence of $W(CO)_6$ also displayed a strong peak of linear adsorbed CO at 2088 cm^{-1} and a weak broad peak of bridging absorbed CO at 1792-1819cm^{-1}. However, no CO peaks were revealed on the sample of Pt nanodendrites.

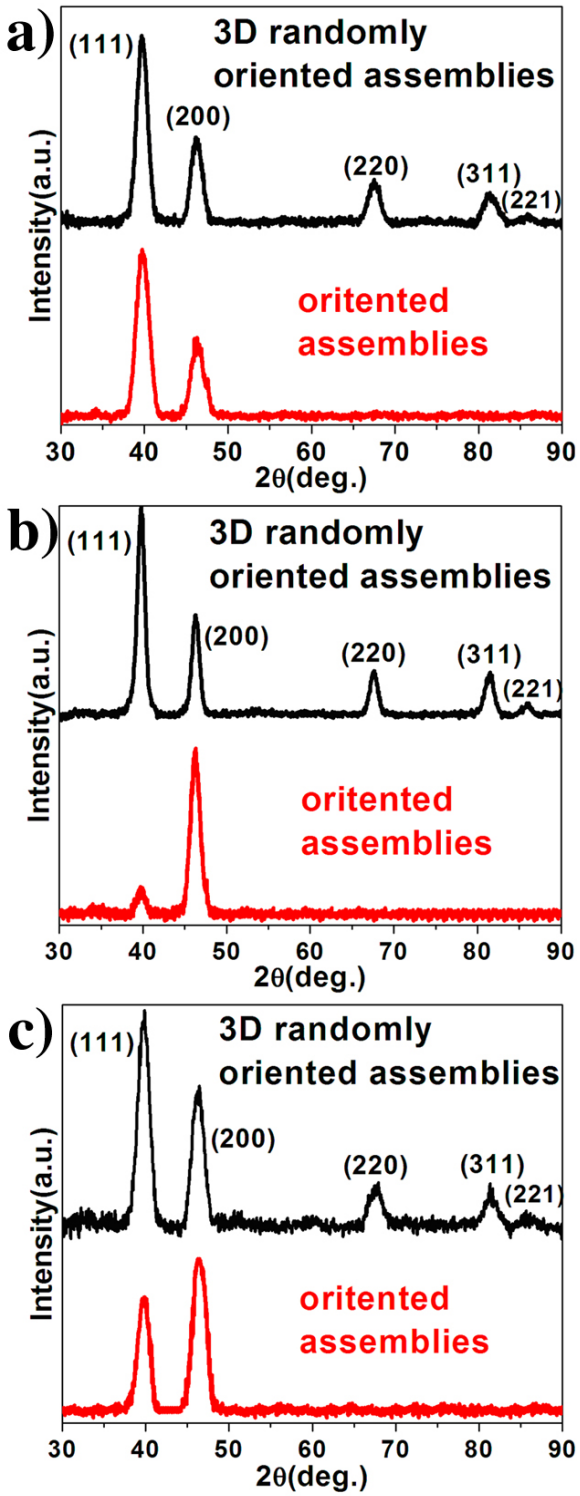

Figure S5. XRD patterns of Pt nanoparticles in pure OAm under (a) CO flow, (b) 1-atm and (c) 2-atm CO.

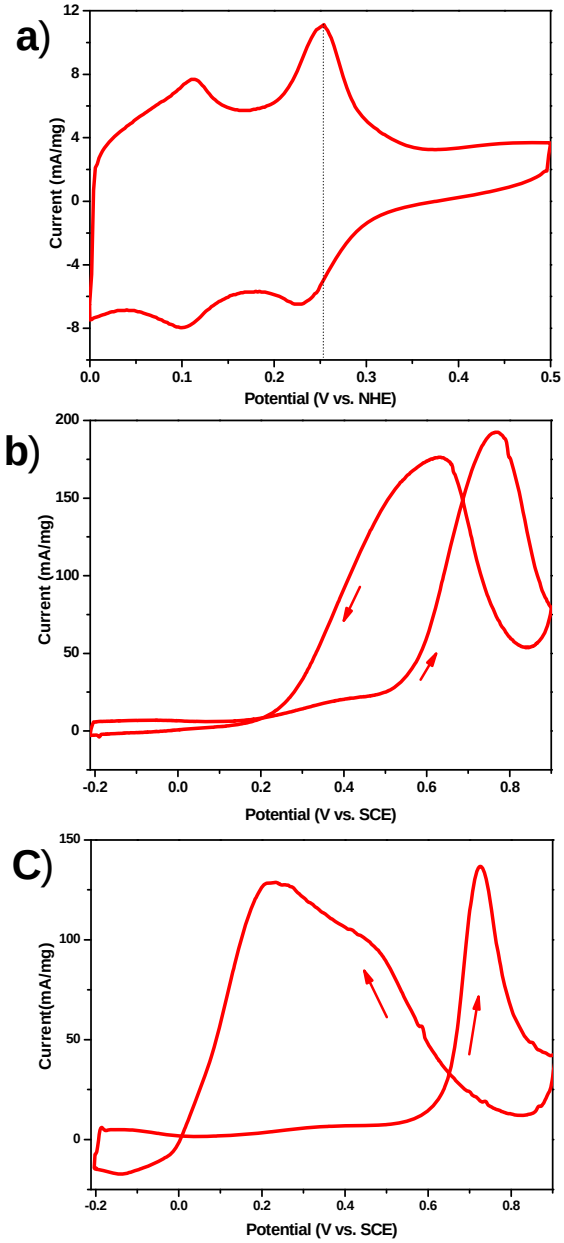

Figure S6. a) CV of the 10.3-nm Pt nanocubes in 0.5 M H_2SO_4. The potential was applied with a scanning rate of 50 mV·s^{-1}. The peak at about 0.25 V originated from the hydrogen desorption on the Pt(100) face.[2,3] CV of 10.3-nm Pt nanocubes in b) 0.5 M H_2SO_4+0.25 M CH_3OH and c) 0.5 M H_2SO_4+ 0.5 M HCOOH solution at a scan rate of 200 mV·s^{-1}. The arrows in the CV curves indicate the direction of the scan. The current was normalized by the weight of catalysts on the electrode.

References

1 J. B. Wu; J. L. Zhang; Z. M. Peng; S. C. Yang; F. T. Wagner; H. Yang, *J. Am. Chem. Soc.* **2010**, *132*, 4984-4985.
2 C. Wang; H. Daimon; Y. Lee; J. Kim; S. H. Sun, *J. Am. Chem. Soc.* **2007**, *129*, 6974-6975.
3 S. Motoo; N. Furuya, *Phys. Chem. Chem. Phys.* **1987**, *91*, 457-461.
4 G. Kresse; J. Hafner, *Phys. Rev. B* **1993**, *48*, 13115-13118.
5 G. Kresse; J. Furthmuller, *Phys. Rev. B* **1996**, *54*, 11169-11186.
6 P. Blochl, *Phys. Rev. B* **1994**, *50*, 17953-17979.
7 G. Kresse; D. Joubert, *Phys. Rev. B* **1999**, *59*, 1758-1775.
8 W. J. Zhang; Y. Liu; R. G. Cao; Z. H. Li; Y. H. Zhang; Y. Tang; K. N. Fan, *J. Am. Chem. Soc.* **2008**, *130*, 15581-15588.